

Observation of Flame Structure in Low Damköhler Number Fields

Manabu FUCHIHATA, Tamio IDA and Yukio MIZUTANI

Department of Mechanical Engineering, School of Science and Engineering, Kinki University

3-4-1 Kowakae, Higashi-Osaka, Osaka 577-8502, Japan

E-mail: fuchihata@mech.kindai.ac.jp

and

Masashi KATSUKI

Department of Mechanical Engineering, Faculty of Engineering, Osaka University

2-1 Yamadaoka, Suita, Osaka 565-0871, Japan

Key Words: Turbulent Premixed Flame, Flame Structure, Distributed Reaction Zone

Introduction

The turbulent premixed flame structure in a low Damköhler number field has been investigated theoretically and experimentally by many researchers [1-10] since Summerfield et al.[1,2] named it distributed reaction zone. The objective of our study is experimentally clarifying the flame structure in low Damköhler number fields, which is needed in combustion modeling. Although such experiments have been done by many researchers, the rigs used in their experiments had no temporal and spatial resolutions needed for observing the phenomena in intense turbulent fields. Takahashi et. al.[10] presented a unique idea for stabilizing low Damköhler number flames in relatively weak turbulent fields by using very lean premixtures. They did not need special measuring system to observe the flame structure because of the long chemical and turbulent time scale nature of the flames. In the present study, we also used very lean premixtures to form low Damköhler number flames and developed an elaborated simultaneous measurement system for observing detailed flame structure.

Experimental Apparatus

The burner used in this study is shown in Fig. 1. This burner is of Bunsen type, having a wide pilot burner port. The inner and outer diameters of central fuel port are 17 mm and 19 mm, respectively. The pilot burner port is arranged around the central fuel port, the width of which is 9 mm. A metal matrix is installed in the pilot burner port. It forms a small pilot flame on each hole and produce a stream of high temperature burnt gas. A special feature of this burner is its wide pilot burner port. The pilot stream prevents the ambient air from influencing the mixing region of main fuel and pilot flows, and enable us to observe the reaction zone stabilized in the mixing region.

Nominal mean flow velocity, u_i , of the central fuel flow, which was a mixture of natural gas and air, were taken to 5 m/s and 3 m/s. Natural gas consisting of 88 % methane, 6 % ethane, 4 % propane and 2 % butane was used. The equivalence ratio, ϕ_i , of the central flow was varied from 0.45 to 0.65 with 0.05 increment. Nominal mean flow velocity, u_o , of the pilot flow, which was stoichiometric mixture of natural gas and air, was taken to 1 m/s. The height, z , of measuring cross sections above the main burner port were 20 mm and 40 mm.

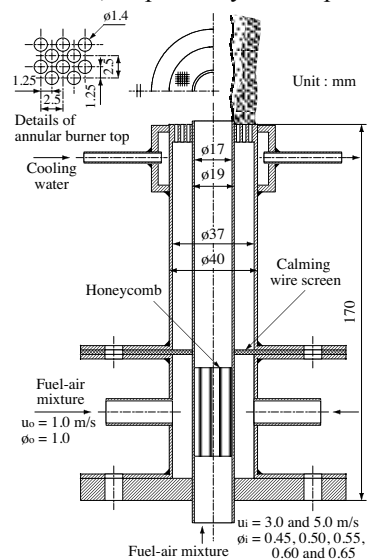


Fig.1 Burner

The lean flammable limit of the mixture with air is around $\phi = 0.55$. A flammable mixture form a conical flame, whereas a mixture leaner than the flammable limit form a cylindrical flame with an open tip on the burner port. The equivalence ratio of the mixture determines its chemical characteristic time, so that, a low Damköhler number flame could be formed even in a weak turbulent field by using a sufficiently lean mixture.

The measuring system used in this study is shown in Fig. 2. The light source for tomography was Ar⁺ CW laser (wave length 514.5 nm and power 3 W). The incident laser beam was expanded to 8 mm diameter during the passage of about 10 m light path, and then it was expanded vertically by the first cylindrical lens and focused horizontally by the second cylindrical lens. The thickness and width of the sheet at the measurement volume were approximately 0.3 mm and 50 mm, respectively. Sequential Mie scattering images of the seeded powder were recorded by the high speed CCD camera (frame rate 9000 frames/s) through an interference filter.

The axial velocity was measured at a point in the laser sheet by LDV. The light source of the LDV was Ar⁺ CW laser (wave length 488 nm and power 1.3 W). The emitted laser beam was conducted to the measurement volume through a manipulator, optical fibers and a transmitter. The beam power at the measurement volume was 60 mW. Doppler burst signal from the measurement volume were condensed by a Cassegrain receiving system [11] free from color aberration. This receiving system also condensed the OH band and CH band emissions from the same measurement volume. The collected light was conducted to a color separator through an optical fiber. The conducted light was separated from each other by dichroic mirrors and purified by interference filters, and then detected by photomultipliers. The detected current signals for OH and CH emissions were transformed into voltage signals by I-V converters and filtered by a low pass filter (cut off frequency 2.5 kHz), then recorded by a personal computer through an A/D converter (sampling time 20 μ s). The detected LDV signal were processed by an LDV signal processor (DANTEC 58N10) and recorded by a personal computer.

The temperature was measured at 0.4 mm downstream of the measurement volume of LDV using a silica coated R-type thermocouple of 25 μ m wire diameter. Voltage signal of the thermocouple was amplified by a preamplifier, and then recorded by an A/D converter together with the frame timing, OH and CH emission signals. Sampling timings of these signals were controlled by a pulse delay generator.

The origin of the measurement area was set at the center of the main burner port. z denotes the vertical height from the main burner port, and r represents the radial distance from the center of the burner port. Measurements were made in and around the reaction zone traversing in r -direction by 1 mm.

Data Processing

Figure 3 shows typical example of image processing. The original picture (a) has roughly three graded gray zones. A luminous spot seen at the center of the original picture (a) is the image of thermocouple junction. We extracted the three graded zones and their boundaries from such images.

The original picture (a) is smoothed spatially, divided into three level zones and noise is eliminated. The manner of decision of the thresholds for gray level classification, which we used in this study, is as follows. At first, the PDF of brightness for all the pixels in the original picture (a) is recorded as (b), which has typically three peaks with two valleys between them. We divide the field into white, gray and dark zones at the valley positions seen in picture (b).

The + marks in Fig. 3(c) represent the measuring points of the thermocouple and Cassegrain probe. A

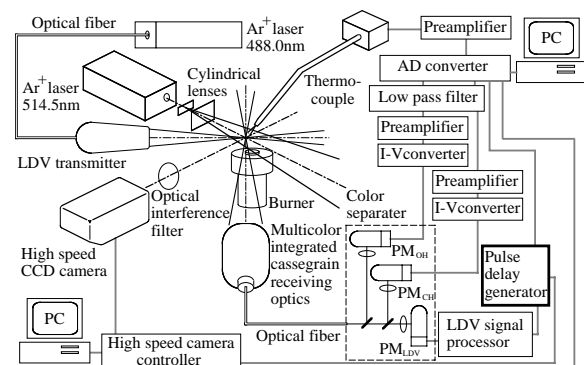


Fig.2 Measuring system

white zone in the image corresponds to the unburned main reactant flow, and the dark zone corresponds to the high temperature burnt gas flow produced by the pilot flames. The gray zone is located between the white and dark zones. A boundary between the white and gray zone is named 'inner boundary' and another boundary between the gray and dark zone is named 'outer boundary'. It is thought that the dark zone indicates the pilot flow region and the white zone indicates the main reactant flow. The gray zone indicates the burned gas of main reactant flow, the mixing region of the main reactant flow and the pilot flow or the coexistent region of those. The structure of the gray zone is the main object of this study and is discussed below in detail.

We deduced the mean flow velocity, turbulent intensity and integral scale of turbulence from the LDV data. Mean flow velocity and turbulent intensity were calculated as the time averaged and rms values, respectively, of the velocity data. Integral scale of turbulence was determined from the time series of discrete velocity data by slot method[12].

Results and Discussions

The conditions of the flames examined in the present study are plotted on Borghi diagram as seen in Fig. 4. These parameters are evaluated just in front of each reaction zone. Fig. 4 indicates that all the combustion conditions are classified into "Distributed reaction zone" and "Well-stirred reactor". We call those conditions "Low Damköhler number fields".

The local mean intensity of OH emission across the reaction zone is shown in Fig. 5 for the cases of the equivalence ratio of main flow $\phi_i = 0.55, 0.60, 0.65$, and $z = 20$ mm and 40 mm. The solid and dotted lines in the figures represent the averaged time fraction, in which the measurement volume stood outside the inner boundary or outside the outer boundary of the gray zone, respectively, obtained from the sequential tomograms. For example, at $r = 7$ mm in Fig. 5(a), the time fractions that the measurement volume stood in white and gray zones are read as about 83 % and 17 %, respectively.

The intensities of OH emission at $z = 20$ mm and 40 mm are plotted as ▲ in Fig. 5. Although relatively intense OH emission appears in the white zone, because the receiving optics do not collect the emission only from its focus, but also from its whole volume of sight, the influence of this is thought to be not so serious around the reaction zone.

Since the OH emission intensity for $\phi_i = 0.55$ is weaker than that for $\phi_i = 0.65$, the reaction intensity for $\phi_i = 0.55$ should be weaker than that for $\phi_i = 0.65$. The profile of mean OH emission for $\phi_i = 0.65$ exhibits a narrow peak just outside the inner boundary, while a low peak slightly close to the outer boundary is taken to be the diffused weak emission from the gray zone for $\phi_i = 0.55$. These results indicate that a thin reaction sheet exists just outside the inner boundary, which should be a wrinkled laminar flame, for $\phi_i = 0.65$. A weak and wide reaction zone exists throughout the gray zone, which resembles so called "distributed reaction" but we call this "pseudo-distributed reaction" in this study, because the reactant does not completely react in this open tip flame, for $\phi_i = 0.55$.

According to the intermediate case for $\phi_i = 0.60$, the emission weaker than its peak intensity appears around (in Fig.

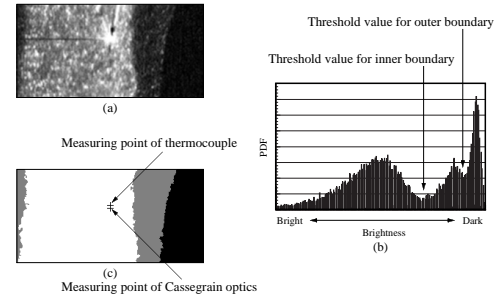


Fig.3 Example of image processing. (a) original picture, (b) PDF of brightness for all the pixels in the original picture and (c) processed picture

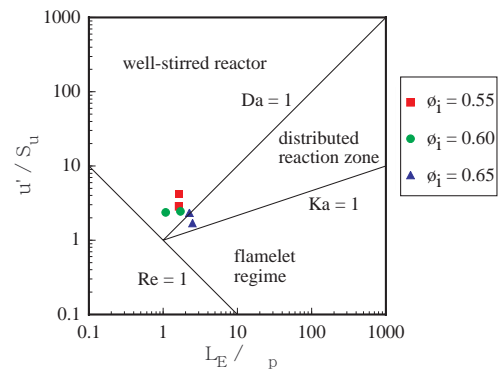


Fig.4 Experimental conditions plotted on Borghi diagram at $u_i = 3.0$ m/s, $z = 20$ mm

5(b)) or just outside (in Fig. 5(e)) the peak of the emission profile. It is supposed that the thin reaction sheet exists amid the pseudo-distributed reaction region for these conditions since the emission intensity at the peak position is comparable to that for $\phi_i = 0.65$.

In order to examine the flame structure at the transition region more precisely, we conditionally sampled the data for $z = 20$ mm and $\phi_i = 0.55, 0.60$ and 0.65 , and made a diagram of temperature fluctuation as shown in Fig. 6. In this diagram, the abscissa denotes the relative distance from the measuring point to the inner boundary and the ordinate denotes the one from the measuring point to the outer boundary. The vertical line, $x_i = 0$, represents the inner boundary and a horizontal line, $x_o = 0$, represents the outer boundary. The first quadrant indicates the region outside both the inner and outer boundaries, which corresponds to the dark zone in the three-gradation pictures, and the third quadrant indicates the region inside both the inner and outer boundaries, which corresponds to the white zone. The fourth quadrant indicates the region inside the outer boundary and outside the inner boundary, which corresponds to the gray zone. The left upper half of the diagram indicates the region where the inner boundary is located outside the outer boundary, which is inhibited. Slant lines $x_i - x_o = w$ ($= const$) indicate constant gray zone width lines, where the gray zone width equals to w . It is supposed that the increment in w mainly corresponds to the extent of progress of mixing and reaction.

Temperature fluctuation is seen throughout the gray zone for $\phi_i = 0.55$, while that is concentrated on the inner boundary for $\phi_i = 0.65$. This also indicates that the flame structure varies from the pseudo-distributed reaction flame, which has micro scale structure, to the wrinkled laminar flame as ϕ_i increases.

Schematic diagrams of flame structure deduced from the examination above are shown in Fig. 7. (a) indicates the structure of an ordinary propagating flame which has a thin reaction zone near the inner boundary, and (c) indicates a pseudo-distributed reaction structure with weak reaction occurring throughout the gray zone. (b), involving two pictures, indicates the flame structure in the transition region observed in this study. In this region, a propagating flame initiates amid the gray zone. The reason why the propagating flame does not initiate around the outer boundary which shows the

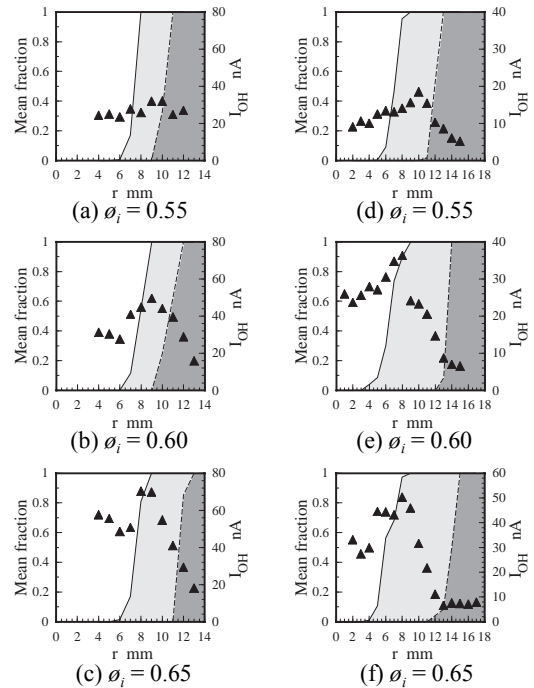


Fig.5 Local mean intensity of OH emission (▲) across the reaction zone and local mean outside-of-boundary fraction. (a), (b) and (c) are for $u_i = 3$ m/s and $z = 20$ mm, and (d), (e) and (f) are for $u_i = 3$ m/s and $z = 40$ mm. (a) and (d) are for $\phi_i = 0.55$, (b) and (e) are for $\phi_i = 0.60$, and (c) and (f) are for $\phi_i = 0.65$.

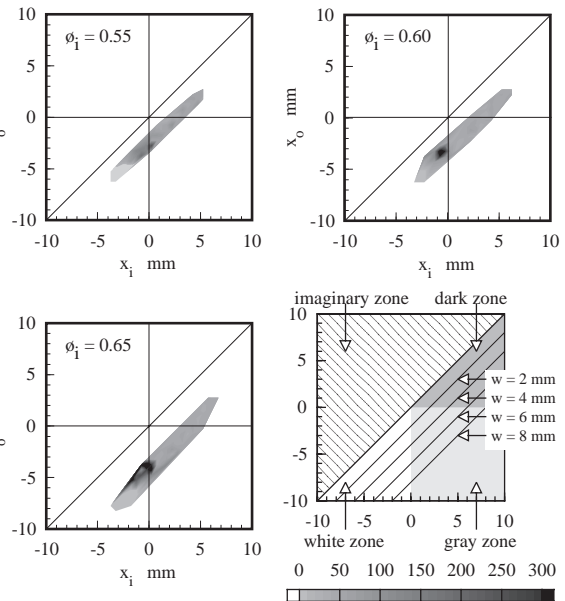


Fig.6 Local rms temperature in terms of relative distance from the measuring point to the inner and outer boundaries at $z = 20$ mm

highest temperature in the gray zone, but initiates amid the gray zone, is that, probably, the reactant is too much diluted by the pilot flow to form a propagating flame around the outer boundary. In that case, a distributed reaction region appears outside the propagating flame. This region is burned out before the propagating flame sufficiently grows and starts to propagate into the main flow, because it is separated from the main reactant flow by the propagating flame.

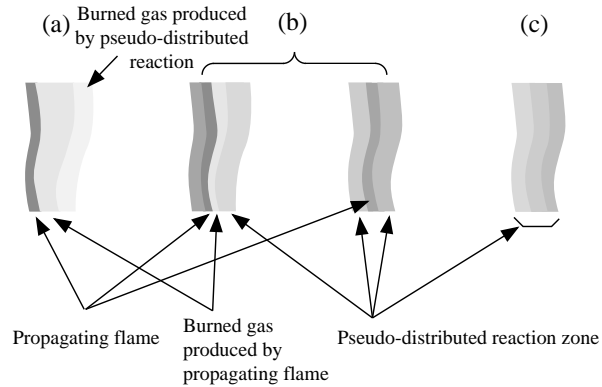


Fig.7 Schematic of flame structure. (a) propagating flame, (b) flame structure in transition region and (c) pseudo-distributed reaction zone

Conclusions

We observed the flame structure of turbulent premixed flames, whose equivalence ratio were around the lean flammable limit, by simultaneously monitoring the laser tomography, chemiluminescence detectors, LDV and a thermocouple data. The conclusions obtained are as follows.

1. When the equivalence ratio of the mixture was close to the flammability limit, a propagating flame did not start from the burner port, but a pseudo-distributed reaction zone was observed there.
2. A propagating flame emerged amid the mixing region between the main reactant flow and the pilot one. A pseudo-distributed reaction zone appeared outside the propagating flame in that case.
3. When the propagating flame sufficiently grew, it started to propagate into the main mixture flow and there is seen no pseudo-distributed reaction zone outside the propagating flame. It was supposed to be a wrinkled laminar flame.

References

- [1] Summerfield, M., Reiter, S.H., Kebely, V. and Mascolo, R.W., *Jet Propulsion*, **24**:254-255 (1954).
- [2] Summerfield, M., Reiter, S.H., Kebely, V. and Mascolo, R.W., *Jet Propulsion*, **25**:377-384 (1955).
- [3] Chomiak, J., *16th Symposium (International) on Combustion*, The Combustion Institute, Pittsburgh, PA, 1976, pp.1665-1673.
- [4] Tabaczynski, R.J., Trinker, F.H. and Shannon, B.A.S., *Combust. Flame*, **39**:111-121 (1980).
- [5] Yoshida, A., *22nd Symposium (International) on Combustion*, The Combustion Institute, Pittsburgh, PA, 1988, pp.1471-1478.
- [6] Yoshida, A., Narisawa, M. and Tsuji, H., *24th Symposium (International) on Combustion*, The Combustion Institute, Pittsburgh, PA, 1992, pp.519-525.
- [7] Damköhler, G., *Z. Elektrochem.*, **46**:601-626 (1940).
- [8] Furukawa, J., Harada, E. and Hirano, T., *23rd Symposium (International) on Combustion*, The Combustion Institute, Pittsburgh, PA, 1990, pp.789-794.
- [9] Buschmann, A., Dinkelacker, F., Schäfer, T., Schäfer, M. and Wolfrum, J., *26th Symposium (International) on Combustion*, The Combustion Institute, Pittsburgh, PA, 1996, pp.437-445.
- [10] Takahashi, T., Katsuki, M. and Mizutani, Y., *Trans. JSME*, **58-547B**:929-936 (1992).
- [11] Wakabayashi, T., Akamatsu, F., Katsuki, M., Mizutani, Y., Ikeda, Y., Kawahara, N. and Nakajima, K., *Trans. JSME*, **64-619B**:925-930 (1998).
- [12] Gaster, M. and Roberts, J.B., *J. Inst. Maths Applics*, **15**:195-216 (1975).